

RESEARCH ARTICLE

WWW.PEGEGOG.NET

Numerical Study of the Effect of Bluff Body Geometry on Drag Force and Flow Pattern

1- Mohammad reza Nazari*, 2- Hamid Farrokhfal, 3- Behrooz Shahriari

1- PhD Student, Neyriz Ghadir Steel Complex(NGHSCO), r.nazari@mut-es.ac.ir

2-Associate Professor, Mechanical Engineering Department, Malek Ashtar University of Technology,
farrokhfal@mut-es.ac.ir

3- Assistant Professor, Mechanical Engineering Department, Malek Ashtar University of Technology,
shahriari@mut-es.ac.ir

Abstract

One of the methods to increase thrust in turbojet engines without increasing engine volume and weight is the use of afterburners. Afterburners are typically used for short durations, such as during takeoff, climb, and reaching maximum flight speed, as well as during maneuvering. One of the main challenges during afterburner operation is flame stability. Bluff bodies are commonly used in turbine engines to ensure flame stability. The presence of a bluff body is essential for maintaining flame stability during afterburner operation; however, it can lead to increased pressure loss when the afterburner is off. This study examined seven different bluff body geometries (five triangular cross-sections, one square cross-section, and one rectangular cross-section). The drag produced by the flame holder and the recirculation zones behind it were analyzed as two key factors in evaluating flame holder performance in both combustion and non-combustion conditions. The bluff body should be designed to achieve a strong recirculation zone while also minimizing pressure loss. The results showed that the bluff body with a square geometry had the highest drag and could lead to flame extinction due to instability in the recirculation zone under varying incoming flow conditions. Investigating the effects of triangular bluff body geometry revealed that modifying sharp edges could significantly reduce drag but might also decrease the length of the recirculation zone, potentially affecting stability. Additionally, creating curvature at the rear of the triangular bluff body could enhance the recirculation zone. The use of V-gutters along with edge modifications can reduce drag while maintaining an adequate recirculation zone length, making this type of bluff body recommended for use.

Keywords

Turbine engines, bluff body, V-gutter, drag, recirculation zone, numerical simulation, flame holder.

1- Introduction

One of the primary challenges in designing air turbine engines is the design of afterburners. Afterburners increase thrust by enhancing the thermal energy of exhaust gases from the nozzle. Bluff bodies are commonly used for flame stability in ramjet engines and afterburners in turbojet and turbofan engines [1]. The bluff body creates a recirculation zone downstream, which contributes to flame stability in combustion systems [2].

How to cite this article: 1- Mohammad reza Nazari*, 2- Hamid Farrokhfal, 3- Behrooz Shahriari. Numerical Study of the Effect of Bluff Body Geometry on Drag Force and Flow Pattern, Vol. 14, No. 4, 2024, 520-535

Source of support: Nil **Conflicts of Interest:** None. **DOI:** 10.48047/pegegog.14.04.44

Received: 12.10.2024

Accepted: 12.11.2024

Published: 01.12.2024

Numerical Study of the Effect of Bluff Body Geometry on Drag Force and Flow Pattern

Fujii et al. conducted studies on non-reactive flow over bluff bodies [3]. Kastner et al. investigated the characteristics of combustion flow behind V-gutters [4]. Simultaneously studying flow behavior during both afterburner on and off states can provide a more comprehensive understanding of bluff body performance. Jie et al. experimentally examined flow fields under both reacting and non-reacting conditions. Results indicated that heat release increases adverse pressure gradients, which can enlarge the recirculation zone size and recirculation rate compared to non-reacting flow fields. Additionally, the V-gutter flame holder demonstrated better fuel/air mixing and larger recirculation than integrated flame holders [5].

Sivakumar et al. studied turbulence intensity and combustion chamber length effects on flame extinction for a bluff body, finding that increased chamber length leads to faster flame extinction[6].

Bluff body geometry significantly affects pressure loss during afterburner shutdown. Changes in bluff body geometry have a direct impact on drag. One way to reduce drag and pressure loss is by decreasing the width of the bluff body [7]. Mohamed et al. showed that modifying the corners of bluff bodies can substantially reduce drag [8]; however, altering the width of the flame holder affects flame stability [9]. Herbert examined the aerodynamic effects of wake and drag coefficients on flame stability boundaries [10]. Although low-pressure drop is considered in the off state of the afterburner, in the on state, pressure reduction is a necessary cost for flame stability and combustion [11]. Additionally, achieving complete combustion at low-pressure drop is not feasible, thus establishing a balance point

between these two is of high importance [12]. The arrangement of flame holders and the blockage ratio also influence drag force and flow pattern. Wright studied the effects of blockage ratio on flame stabilization [13]. Furthermore, the arrangement of flame holders should be such that it not only provides stable combustion but also does not increase blockage and consequently pressure drop [14-15]. In addition to the above factors, the angle of V-gutters also affects flow behavior. Yong et al. numerically examined the effects of the internal apex angle of triangular bluff bodies on turbulent combustion flow and thermal field in a channel. The apex angle varied from 45 degrees to 150 degrees. Results showed that as the apex angle of the bluff body increased, the flame width increased, which in turn enhanced the chamber volume heat release ratio and improved flame stability [16]. Boopathi investigated flame stability for different apex angles of V-gutters. They experimentally studied flame stability under four different inlet pressure conditions and six V-gutter apex angles. Results indicated that flame stability was achieved across the entire pressure range when the V-gutter apex angle was either 60 degrees or 90 degrees [17]. Aiwu et al. conducted a profound study on the effect of bluff body shape, inlet velocities, and equivalence ratios on blow-off limits, combustion processes, flame stabilization, and heat transfer. It was shown that flame stabilization significantly depends on the recirculation zone and flame stretching behind the flame holder [18-19-20-21].

In this study, numerical simulations for both combustion and non-combustion states were performed on several bluff bodies with different geometries. Flow behavior, recirculation area, and drag were examined as

Numerical Study of the Effect of Bluff Body Geometry on Drag Force and Flow Pattern

key performance parameters. Results indicated that bluff body geometries with triangular cross-sections exhibited the best performance. Additionally, removing sharp

points and increasing the internal angle of triangular sections can not only reduce drag but also increase the length of the recirculation area.

2- Governing Equations

The mass conservation equation is one of the most important equations for analyzing species reactions. This equation is defined as follows:

$$\frac{\partial \rho}{\partial t} + \nabla \cdot \rho u = 0 \quad (1)$$

The conservation of momentum equation can be expressed as the following equation:

$$\rho \left(\frac{\partial u}{\partial t} + \nabla u \cdot u \right) = -\nabla p + \rho g + \nabla \cdot \mu \nabla (u + u^T) + \sigma k \delta \varphi (\nabla \varphi) \quad (2)$$

Additionally, to simulate combustion, it is necessary to use the energy conservation equation:

$$\begin{aligned} \frac{\partial}{\partial t} (\rho E) + \nabla \cdot (\vec{v} (\rho E + p)) \\ = \nabla \cdot \left(k_{eff} \nabla T \right. \\ \left. - \sum_j h_j \vec{J}_j + (\vec{\tau}_{eff} \cdot \vec{v}) + Sh \right) \end{aligned} \quad (3)$$

where:

$$E = h - \frac{p}{\rho} + \frac{u_i^2}{2} \quad (4)$$

For premixed combustion, Equation (3) can be rewritten as:

$$\frac{\partial}{\partial t} (\rho E) + \nabla \cdot (\rho \vec{v} H) = \nabla \cdot \left(\frac{K_t}{C_p} \nabla H \right) + S \quad (5)$$

where H is obtained from relation (6):

Numerical Study of the Effect of Bluff Body Geometry on Drag Force and Flow Pattern

$$H = \sum_j Y_j H_j \quad (6)$$

$$H_j = \int_{T_{ref,j}}^T C_{p,j} dT + h_j^0(T_{ref,j}) \quad (7)$$

In this work, the *k- ω SST* model was used for simulating turbulent flow. One of the features of this model compared to the *standard k- ω* model is its limitation correction for vortex viscosity growth in rapidly deforming flows. In this model, turbulence kinetic energy (*k*) and specific dissipation rate (ω) are obtained from the following equations:

$$\frac{\partial k}{\partial t} + U_j \frac{\partial k}{\partial x_j} = \frac{\partial}{\partial x_j} \left[(v + \sigma_k v_T) \frac{\partial k}{\partial x_j} \right] + G_k \quad (8)$$

$$\begin{aligned} \frac{\partial \omega}{\partial t} + U_j \frac{\partial \omega}{\partial x_j} = & \frac{\partial}{\partial x_j} \left[(v + \sigma_\omega v_T) \frac{\partial \omega}{\partial x_j} \right] \\ & + G_\omega - \beta \omega^2 + D_\omega \end{aligned} \quad (9)$$

In this relation, G_k is the turbulence kinetic energy created due to velocity gradients. G_ω represents the generation of ω , and the last term of the equation indicates the transverse diffusion term (D_ω) [22].

3- Validation:

To validate the employed model, numerical results must be compared with experimental data. The validation case is the Volvo combustion system, which includes a triangular bluff body placed within a rectangular channel [23]. Numerous experimental [24-25] and numerical [26-27-28] studies have been based on Volvo's work. Figure 1 shows a schematic of the Volvo combustion system. The holder is in the shape of an equilateral triangle with each side measuring $D=4$ cm. The fuel used is propane mixed with air at a temperature of 288 K. Other input conditions for the problem are shown in Table 1.

Table 1: Inlet flow conditions for the Volvo chamber

Value	Parameter
0.2083kg/s	Mass flow rate (fuel-air mixture)
17.3 m/s	Velocity
288 k	Temperature
0.65	Equivalence ratio

Numerical Study of the Effect of Bluff Body Geometry on Drag Force and Flow Pattern

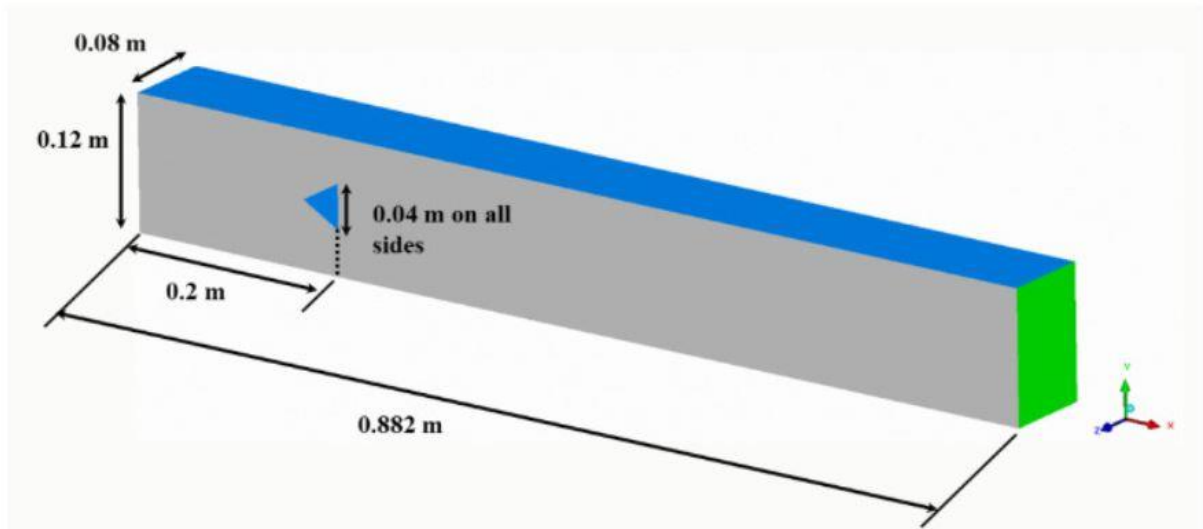


Figure 1: Volvo Bluff Body MVP Workshop Simulation Set Up [30]

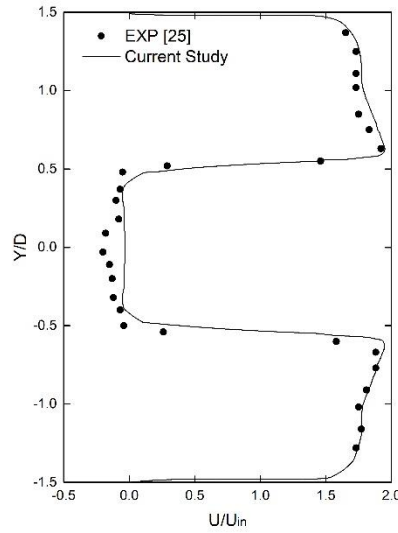
A mass flow rate boundary condition is considered for the inlet and a constant pressure condition for the outlet. In this work, the $k-\omega$ shear stress transport (SST) modeling approach was used for turbulence, which has been confirmed by several studies as a suitable choice for bluff body simulations [29-30]. The simulation was conducted in two dimensions, and the simulation domain is shown in Figure 2.



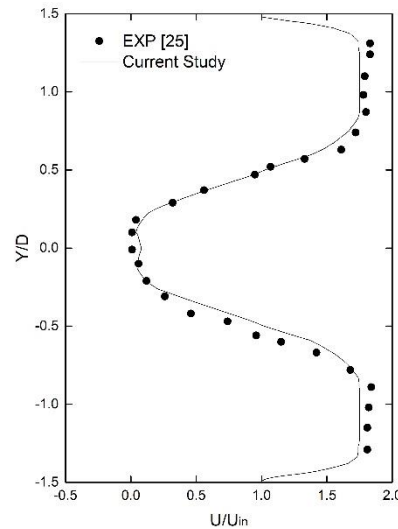
Figure 2: CFD Model Geometry

Simulations were performed in both non-reacting and reacting flow states, and the results were analyzed at various sections along the rectangular channel. Figure 3 shows the average velocity profile at the sections $x/D=0.375$ and $x/D=0.375$ along the flame. The results indicate that the numerical solution has acceptable accuracy compared to experimental results, but there is a slight difference in estimating the vortex length behind the bluff body due to simplifications made in the simulation. The results show that near the walls, the velocity is nearly zero, and as one approaches the centerline, the velocity initially increases and then decreases again due to recirculating flows.

Numerical Study of the Effect of Bluff Body Geometry on Drag Force and Flow Pattern



(a) $x/D=0.375$

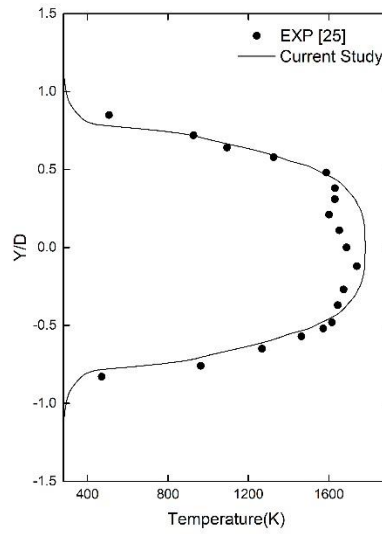


(b) $x/D=3.75$

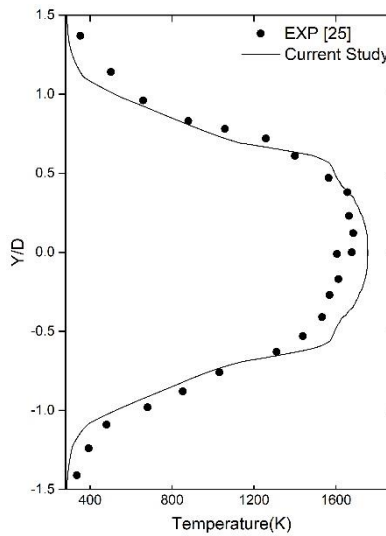
Figure 3: Dimensionless average velocity profile at different axial sections along the flame for numerical and experimental results.

In Figure 4, the average temperature profile for the sections $x/D=0.375$ and $x/D=0.375$ along the flame is shown for the reacting state. The results indicate that after flame formation in the region behind the bluff body, the temperature increases. As one moves away from the bluff body (from section $x/D=0.375$ to section $x/D=0.375$), the flame expands, causing an increase in temperature near the walls as well. The numerical solution shows good agreement with experimental results, indicating the validity of the model chosen for simulation.

Numerical Study of the Effect of Bluff Body Geometry on Drag Force and Flow Pattern



(a)= $x/D=3.75$



(b)= $x/D=9.75$

Figure 4: Average temperature profile at different axial sections along the flame for numerical and experimental results.

4- Case Study

In this work, to determine the effect of bluff body geometry on flow behavior, drag, and recirculation area, various geometries with different cross-sections were used. For this purpose,

Numerical Study of the Effect of Bluff Body Geometry on Drag Force and Flow Pattern

seven different geometries were employed, all maintaining a constant bluff body width. Figure 5 shows the cross-sections of the bluff bodies studied in this research.

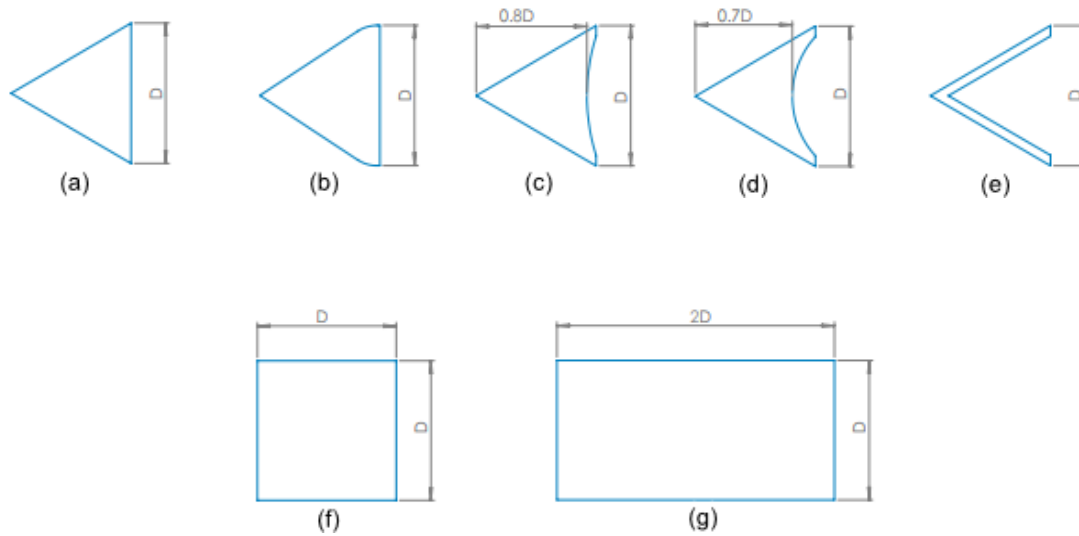


Figure 5: Cross-section of bluff bodies used in this research.

Geometry **a** is an equilateral triangle, which is the same as the Volvo geometry. Geometries **b**, **c**, and **d** are similar to geometry **a**; however, in geometry **b**, sharp points on both sides have been removed, while geometries **c** and **d** have curved surfaces of different sizes created within their internal section to observe their effect on the recirculation area. Geometry **e** is a V-gutter with a thickness of 5 mm that has dimensions exactly similar to geometry **a**. Geometries **f** and **g** have completely different cross-sections; unlike previous geometries, the flow does not strike an angled surface. Section **f** is a square with the same constant width **D**, and section **g** is a rectangle with width **D** and length **2D**.

5- Results

To determine the geometric variations in flow characteristics, simulations were conducted in both reacting and non-reacting states. Figure 6 shows the velocity contour for different sections. The results of the flow pattern indicate that while maintaining a constant flame width of the holder, removing sharp edges from triangular bluff bodies (geometry **b**) reduces the width of the recirculation area behind the bluff body, resulting in an increase in effective flow area and a decrease in velocity on both sides of the bluff body; however, for other triangular cross-sections, there was not much difference in the overall flow pattern. Changing the bluff body geometry from triangular to square significantly alters the flow pattern. Firstly, a stagnation point forms at the front of the bluff body, and also, flow immediately separates after passing over the front edge of the body, initiating recirculating flows from its leading edge.

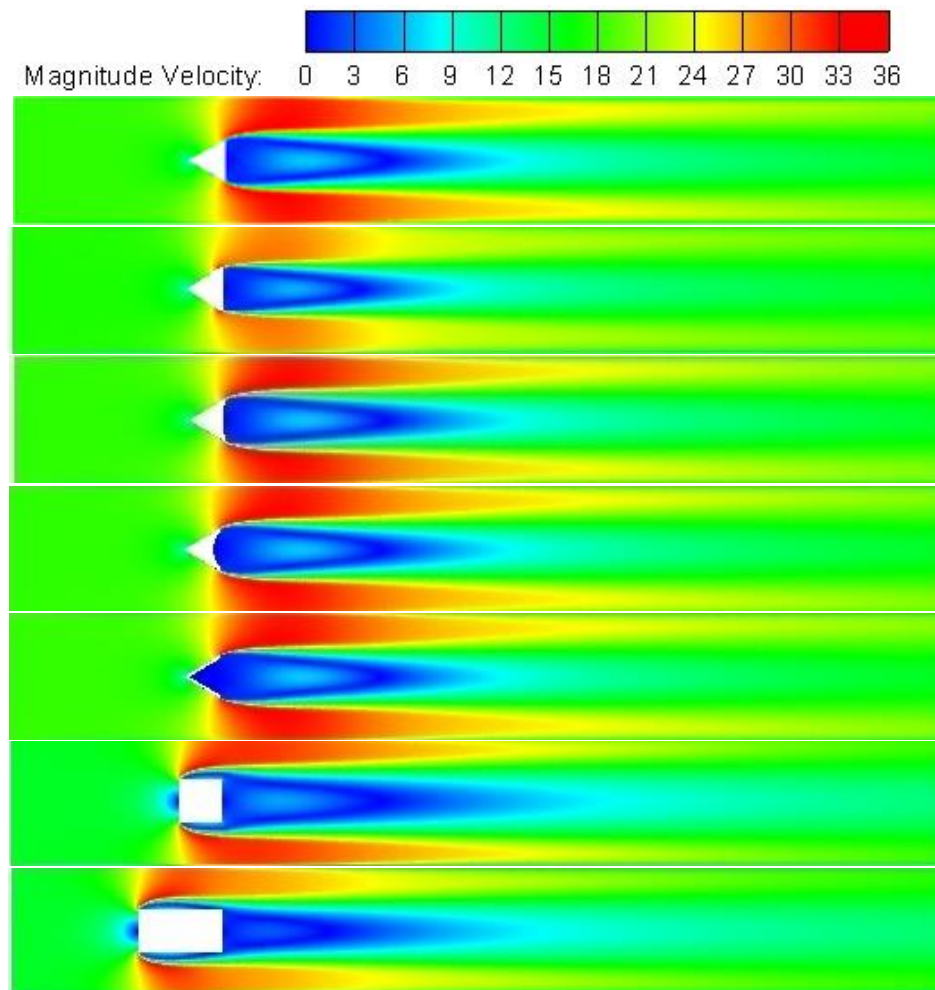


Figure 6: Velocity contour for different cross-sections in a non-reacting state.

In Figure 7, the velocity contour along with streamlines is shown, and in Figure 8, the percentage change in drag for different sections is presented. The results indicate that at all sections behind the bluff body, two pairs of vortices are formed. By comparing the changes in drag and vortex length between sections **a** and **b**, it can be concluded that modifying the sharp edges of the triangular cross-section reduces the length of the vortices, while the drag decreases

significantly by about 31%. In geometries **c** to **e**, the length of the vortices remains approximately constant but has increased compared to section **a**. Additionally, in geometry **c**, the recirculating flow is attached to the bluff body, but with an increase in indentation within the bluff body (according to geometry **e**), the vortex flow no longer adheres to the body. Furthermore, drag increases for sections **c** and **d** but decreases for section **e**. As expected, the vortex flow for

Numerical Study of the Effect of Bluff Body Geometry on Drag Force and Flow Pattern

square and rectangular sections differs, with flow separation occurring immediately after the front edge. Also, the length of the recirculating area behind the rectangular bluff body significantly decreases due to the weakening of the flow. Among all examined sections, the square section has the longest

recirculating area and the highest drag, while the rectangular section, despite having high drag, has the smallest recirculating area. This sudden increase in drag for square and rectangular sections results from a significant pressure difference at the front and back of the geometry.

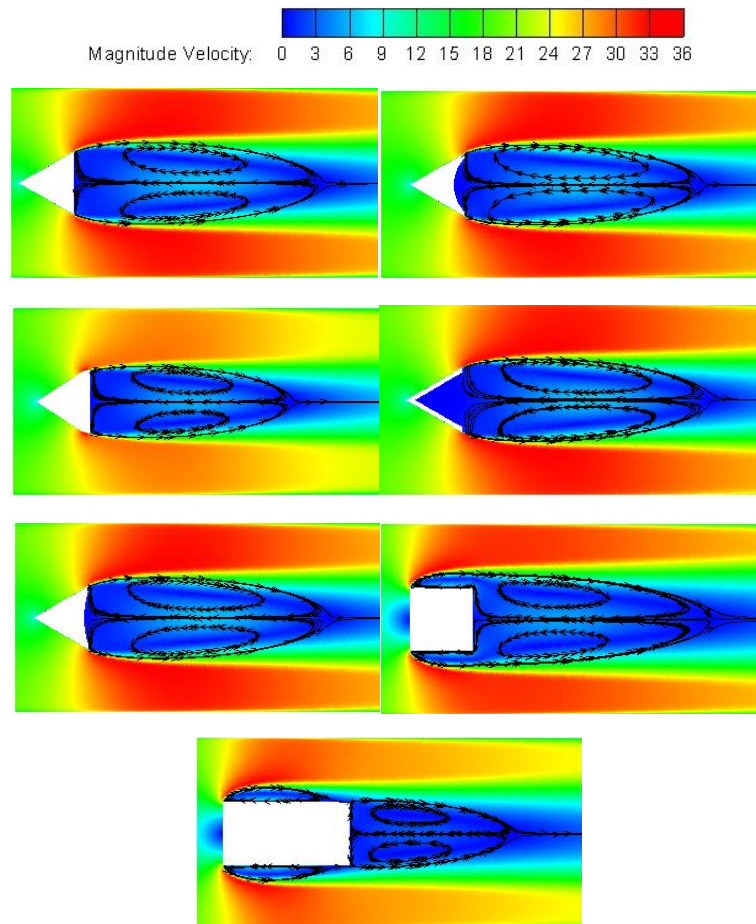


Figure 7: Velocity contour along with streamlines for different cross-sections in a non-reacting state.

Numerical Study of the Effect of Bluff Body Geometry on Drag Force and Flow Pattern

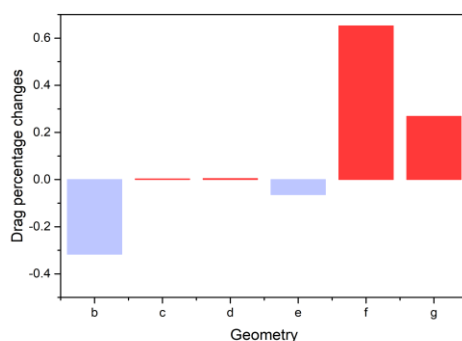
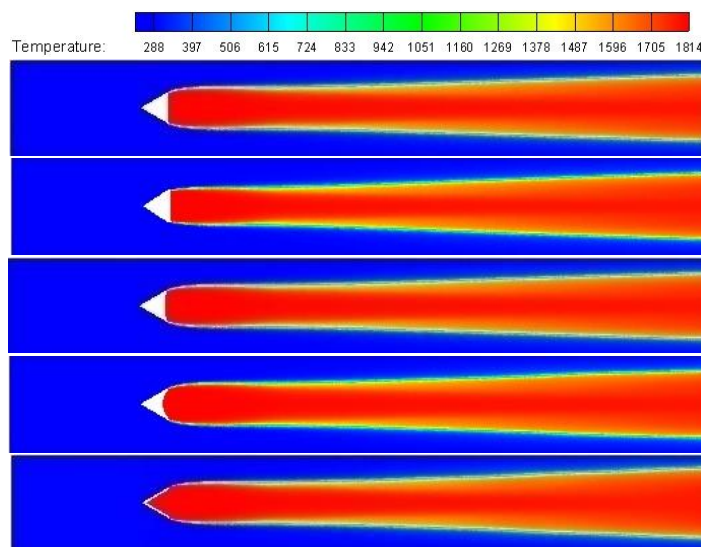


Figure 8: Percentage change in drag for different sections.

In this section, the flow pattern in the combustion state has been analyzed. In Figure 9, the temperature contour for various sections in the combustion state is presented. The results show that the flame shape for triangular sections (a to e) is nearly identical, except for section **b**, where the removal of sharp edge points from the triangular cross-section allows for better flow alignment with the bluff body, thereby reducing the initial width of the flame. The angle of flame spread is also independent of fuel type, inlet flow

velocity, and equivalence ratio [31]. Moreover, the angle of flame spread depends on the turbulence of the flow and the temperature of the inlet flow. Therefore, it is observed that for all triangular sections, the angle of flame spread remains constant. According to the results, a flame forms immediately after all sections of the bluff body; however, for section **f**, due to the initiation of recirculating flow from the initial plane of geometry, flame initiation occurs from the leading edge of the body.



Numerical Study of the Effect of Bluff Body Geometry on Drag Force and Flow Pattern

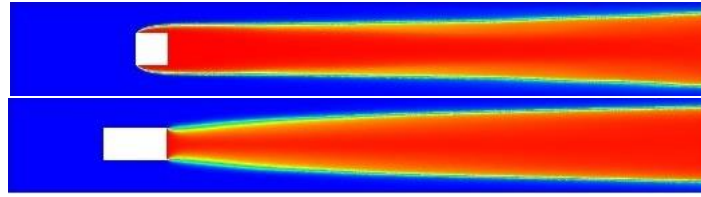
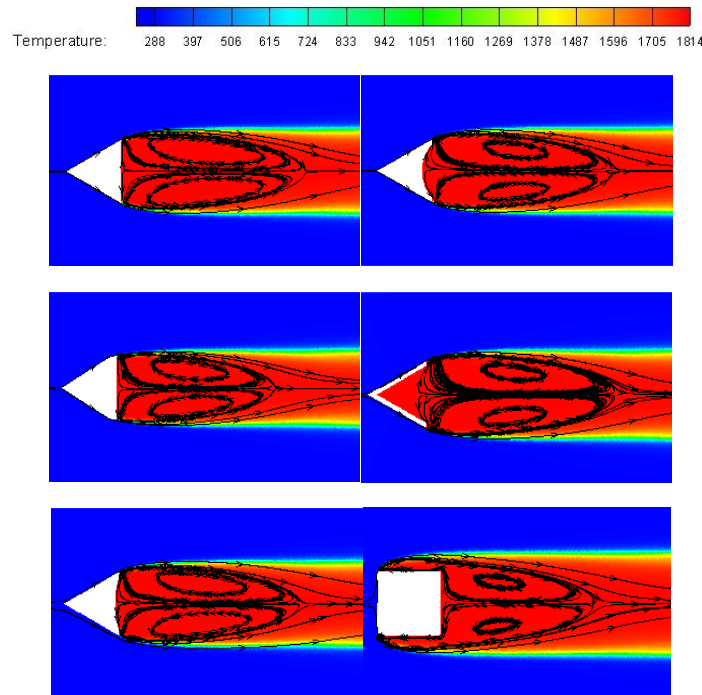


Figure 9: Temperature contour for different cross-sections in a reacting state.

In Figure 10, the temperature contour along with streamlines in the combustion state is shown. Similar to the cold state, two vortices form immediately behind the bluff body. In section **b**, similar to the cold state, both the width and length of vortices have decreased compared to section **a**. In sections **c** to **e**, the recirculating flow behind the bluff body forms a stronger flow compared to the cold state and penetrates more into the empty area behind the bluff body; additionally, the length of the recirculating area has increased compared to section **a**. Therefore, for better stability, it is recommended to use section **e** since it creates the largest recirculating area in downstream flow. In section **f**, vortices

form from the leading edge of the flow and continue to extend behind the body without interruption. However, in section **g**, flow separation occurs at the leading edge; as the flow passes over the body, it gets another chance to adhere to it, which weakens vortex formation. Consequently, unlike section **f**, not only does combustion not initiate from the leading edge of this body but also significantly reduces vortex formation behind it. Although section **f** has a suitable length for the recirculating area, it may exhibit behavior similar to section **g** during actual flight due to flow fluctuations under varying flight conditions; thus, stability may be greatly reduced.



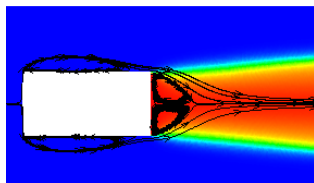


Figure 10: Temperature contour along with streamlines for different cross-sections in reacting state.

5- Conclusion:

This paper examined the impact of different geometries on the flow behavior in both lit and unlit afterburners. The characteristics of the recirculating area and drag were evaluated as two important factors in flame stability and pressure loss, leading to the following results:

1. In triangular cross-sections, by removing sharp geometric points (according to geometry b), the drag force decreased significantly by about 31% compared to the baseline geometry, which represents the highest reduction in drag compared to other sections. On the other hand, the length and width of the recirculating area slightly decreased compared to the baseline geometry. Therefore, it is recommended that if the aircraft requires the use of an afterburner for only a limited time, this section should be used to reduce pressure loss.

2. By changing the geometry behind the bluff body (sections c and d), drag slightly increases, but the recirculating area also increases, which enhances flame stability.

3. The use of a V-gutter has resulted in a 6% reduction in drag compared to the baseline geometry, while also increasing the length of the recirculating area. Therefore, it is

recommended that this section be used if flame stability is a priority.

4. The square cross-section exhibited the highest drag compared to other sections, with drag increasing by 63% compared to the baseline triangular section. Moreover, in the square section, the flame forms well, and the size of the vortices is adequate. However, due to fluctuations in the incoming flow, it may behave similarly to the rectangular section, leading to flame instability; in this case, we would experience the highest drag along with a high risk of flame extinction.

5. The rectangular cross-section not only increases drag by 24% compared to the baseline triangular section but also significantly reduces the length of the recirculating area; thus, this rectangular section is not recommended.

6. The results showed that the length of the recirculating area behind the bluff body increases with increasing drag, but this relationship is not linear. Therefore, by modifying the sharp points of the V-gutter geometry (geometry e), it is possible to achieve the longest recirculating area with the least drag.

References

Numerical Study of the Effect of Bluff Body Geometry on Drag Force and Flow Pattern

- [1] Bush, Scott M., and Ephraim J. Gutmark. Reacting and nonreacting flowfields of a V-gutter stabilized flame. *AIAA journal* 45.3 (2007): 662-672, <https://doi.org/10.2514/1.22655>
- [2] Santosh J. S, Sajjad H, Tim L. Lean blowoff of bluff body stabilized flames Scaling and dynamics. *Progress in Energy and Combustion Science* 35 (2009) 98–120, <https://doi.org/10.1016/j.pecs.2008.07.003>
- [3] S. Fujii, M. Gomi, and K. Eguchi, Cold flow tests of a bluffbody flame stabilizer. *Journal of Fluids Engineering ASME*, vol. 100, no. 3, pp. 323–332, 1978. <https://doi.org/10.1115/1.3448673>
- [4] D. R. Cuppoletti, J. Kastner, J. Reed, and E. J. Gutmark, High frequency combustion instabilities with radial V-gutter flameholders. in *Proceedings of the 47th AIAA Aerospace Sciences Meeting including the New Horizons Forum and Aerospace Exposition*, AIAA Paper no. 2009-1176, January 2009. <https://doi.org/10.2514/6.2009-1176>
- [5] Jie L, Tao X, Bolun S, Wenyan S, Chen H. Experimental study on flow field and combustion characteristics of V-gutter and integrated flameholders, *Int Turbo Jet Eng* 2024:aop. <https://doi.org/10.1515/tjj-2024-0021>
- [6] Sivakumar and Chakravarthy. Experimental investigation of the acoustic field in a bluff-body combustor. *Int J Aeroacoust* 2008;7(3–4):267–99. <https://doi.org/10.1260/1475-472X.7.3.267>
- [7] S. Nakanishi, W. Velie, W.L. Bryant, An investigation of effects of flame-holder gutter shape on afterburner performance, *Tech. Rep.* Arch. Image Libr.(1954). <https://ntrs.nasa.gov/citations/19930088008>
- [8] Mohamed IK, Aissa WA. Effect of corner modification on two-dimensional turbulent flow around a square cylinder with incidence. *J Eng Sci, Assiut Univ* 2016;44:91–102 <http://dx.doi.org/10.21608/jesaun.2016.117589>
- [9] K.V.L. Rao, A.H. Lefebvre, Flame blowoff studies using large scale flameholders, *J. Eng. Power.* 104 (1982) 853, <https://doi.org/10.1115/1.3227355>.
- [10] Herbert MV. Aerodynamics influences on flame stability. *Progress in Combustion Science and Technology* 1980:61–109. <https://doi.org/10.1016/B978-0-08-009468-7.50007-1>
- [11] Rizk N K. Lefebvre A H. The relationship between flame stability and drag of bluff-body flame-holders. *Journal of propulsion and power*, 1986, 2(4):361-365. <https://doi.org/10.2514/3.22895>
- [12] Ma Wenjie, Yang Maolin, Jin Jie, et al. Research on combustion performance of the aspirated edge blowing mixture cutain flameholder. *AIAA* 2009-5293. <https://doi.org/10.2514/6.2009-5293>
- [13] Wright FH. Bluff-body flame stabilization: blockage effects. *Combust Flame* 1959;26:319–37. [https://doi.org/10.1016/0010-2180\(59\)90035-5](https://doi.org/10.1016/0010-2180(59)90035-5).
- [14] Jeffery A L. Barry V K, Torence P B, et al. Development needs for advanced afterburner design. *AIAA* 2004-4192. <https://doi.org/10.2514/6.2004-4192>

Numerical Study of the Effect of Bluff Body Geometry on Drag Force and Flow Pattern

[15] Houshang B E. Overview of gas turbine augmentor design, operation and combustion oscillation. AIAA 2006-4916.

<https://doi.org/10.2514/6.2006-4916>

[16] Yang G, Jin H, Bai N. A numerical study on premixed bluff body flame of different bluff apex angle. Mathem Problems Eng 2013;1–9. 272567

<http://dx.doi.org/10.1155/2013/272567>

[17] Boopathi S, Maran P. Effect of air pressure and gutter angle on flame, stability and DeZubay number for methane-air combustion. Int J Turbo Jet Engines 2016;34

<https://doi.org/10.1515/tjj-2016-0018>

[18] Aiwu, F., et al., Effect of Bluff Body Shape on the Blow-off Limit of Hydrogen/Air Flame in a Planar Micro-Combustor, Applied Thermal Engineering, 62 (2014), 1, pp. 13-19.

<https://doi.org/10.1016/j.applthermaleng.2013.09.010>

[19] Aiwu, F., et al., Interactions between Heat Transfer, Flow Field and Flame Stabilization in a Micro-Combustor with a Bluff Body, Int. Journal of Heat and Mass Transfer, 66 (2013), Nov., pp. 72-79.

<https://doi.org/10.1016/j.ijheatmasstransfer.2013.07.024>

[20] Jianlong, W., et al., Experimental and Numerical Investigation on Combustion Characteristics of Premixed Hydrogen/Air Flame in a Micro-Combustor with a Bluff Body, International Journal of Hydrogen Energy, 37 (2012), 24, pp. 19190-19197.

<https://doi.org/10.1016/j.ijhydene.2012.09.154>

[21] Aiwu, F., et al., The Effect of the Blockage Ratio on the Blow-off Limit of a Hydrogen/Air Flame in a Planar Micro-Combustor with a Bluff Body, Int. J. of Hydrogen Energy, 38 (2013), 26, pp. 11438-11445.

<https://doi.org/10.1016/j.ijhydene.2013.06.100>

[22] Trotter Cebeci, (2003), “Turbulence Models and Their Application”, Horizons Publishing Inc, pp 10 13 .

[23] Comer, A. et al, Model Validation Propulsion (MVP) Workshop test case description.

<http://web.stanford.edu/group/ihmegroup/cgi-bin/mvpws/development>

[24] Sjunnesson A., Olovsson S. and Sjöblom B., “Validation Rig – A Tool for Flame Studies”, International Society for Airbreathing Engines Conference, ISABE-91-7038, Nottingham, United Kingdom, 1991.

<https://community.apan.org/wg/afrlwg/mvpws/p/experimental-data>

[25] Sjunnesson A., Nelsson C and Max E., “LDA Measurements of Velocities and Turbulence in a Bluff Body Stabilized Flame”, Fourth International Conference on Laser Anemometry – Advances and Application, ASME, Cleveland, OH, 1991.

[26] ghani, A., Poinot, T., Gicquel, L., and Staffelbach, G. “LES of longitudinal and transverse self-excited combustion instabilities in a bluff-body stabilized turbulent premixed flame.” Combustion and Flame, Vol. 162, 2015, pp. 4075-83.

<https://doi.org/10.1016/j.combustflame.2015.08.024>

[27] Comer, A. L ., Huang, C., Rankin, B., Harvazinski, M., and Sankaran, V. “Modeling and Simulation of Bluff Body Stabilized Turbulent Premixed Flames,” 54th AIAA Aerospace Sciences Meeting, AIAA 2016-1936, San Diego, CA, 2016.

<https://doi.org/10.2514/6.2016-1936>

[28] Scott A. Drennan ,Gaurav Kumar, Rankin, and Shuaishuai Liu. “Developing Grid-Convergent LES Simulations of Augmentor Combustion with Automatic Meshing and Adaptive Mesh Refinement,” 55th AIAA Aerospace Sciences Meeting, AIAA 9-13,Grapevine , Texas, 2017.

<https://doi.org/10.2514/6.2017-1574>

[29] Menter FR. Two-equation eddy-viscosity turbulence models for engineering applications. AIAA J 1994;32:1598–605.

<https://doi.org/10.2514/3.12149>

[30] Menter FR. Zonal two-equation $k-\omega$ turbulence model for aerodynamic flows. In: AIAA paper 1993–2906; 1993.

<https://doi.org/10.2514/6.1993-2906>

[31] E. Zukoski, Aerothermodynamics of Aircraft Engine Components, AIAA, 1985.